

Empirical formulations for evaluation of across-wind dynamic loads on rectangular tall buildings

Young-Cheol Ha*

Department of Architecture, Kumoh National Institute of Technology, Gumi, South Korea

(Received September 28, 2011, Revised February 1, 2012, Accepted July 7, 2012)

Abstract. This study is aimed at formulating an empirical equation for the across-wind fluctuating moment and spectral density coefficient, which are needed to estimate the across-wind dynamic responses of tall buildings, as a function of the side ratios of buildings. In order to estimate an empirical formula, wind tunnel tests were conducted on aero-elastic models of the rectangular prisms with various aspect and side ratios in turbulent boundary layer flows. In this paper, criteria for the across-wind fluctuating moment and spectral density are briefly discussed and the results are analyzed mainly as a function of the side ratios of the buildings. Finally, empirical formulas for the across-wind fluctuating moment coefficient and spectral density coefficient according to variation of the aspect ratio are proposed.

Keywords: tall building; across-wind load; aspect ratio; side ratio; fluctuating moment; power spectral density

1. Introduction

The analytical methods for the along-wind response (the gust factor approach or spectral modal analysis) are applicable to most prismatic structures (Davenport 1962, Vickery 1966). These are possible mainly because the along-wind response of most structures originates almost entirely from the action of the wind gustiness of the longitudinal component of the wind velocity. The power spectral density of longitudinal wind velocity has a wide-band shape and does not change its shape significantly according to terrain conditions, heights above ground and wind speeds. Therefore, analytical methods using spectral and spatial correlation considerations to predict the along-wind response have become highly developed, and are included in a number of wind loading codes (AIJ 2004, KBC 2009, NBC 2005).

In contrast, the across-wind forcing mechanism has proved to be so complex that as yet, there is no generalized analytical method available for calculating the across-wind responses of such structures. This is because the across-wind power spectral density changes significantly with aspect ratio, side ratio, terrain conditions, wind speed and the dynamic characteristics of the structures. In particular, the vortex shedding occurring to the rear of a building is strongly affected by the aspect and side ratios of the building. For these reason, it is very difficult to generalize the

* Corresponding Author, Professor, E-mail: ycha@kumoh.ac.kr

across-wind force spectral density with an empirical equation. Many wind tunnel tests for vortex-induced vibration have been carried out for rectangular prisms and various interesting features of vortex-induced vibrations have already been found (Vickery 1972, Melbourne 1975, Kareem 1989, Kawai 1992, Ha 2002). However, attempts to introduce an empirical equation for the across-wind force spectral density are rare. Liang *et al.* (2002, 2005) conducted wind pressure tests for models having four types of side ratio ($D/B=1, 2, 3$ and 4 where, B is the breadth of the building and D is the depth), and proposed a mathematical model for the across-wind force spectral density as a function of the side ratio. Lin *et al.* (2005) conducted wind pressure test for nine models with different rectangular cross-sections, and investigated local wind forces spectra on along-wind and on across-wind. The effects of three parameters, elevation, aspect ratio, and side ratio, on bluff body flow and on local wind force are discussed. Ha (2004) conducted high-frequency force balance (HFFB) tests for model with thirteen types of side ratio, and proposed empirical formulas for the across-wind force spectral density as a function of side ratio. Ha *et al.* (2005) conducted HFFB tests for models having thirteen types of side ratio and for four different conditions of ground-surface roughness, and found that across-wind force spectral density is little affected by the ground-surface roughness. QUAN *et al.* (2006), based on the results of the across-wind aerodynamic forces and aero dynamic damping of high-rise buildings, developed a new analytical method of for across-wind responses and corresponding equivalent static wind loads of high-rise buildings. Kim *et al.* (2008) conducted wind tunnel test for an aero-elastic tapered model of a tall building and investigated the effect of tapering on reducing the rms across-wind displacements. Nan *et al.* (2007, 2008), based on the occurrence mechanism of pressure fluctuation and Taylor assumption in turbulence, derived analytical solution of spectral density function of pressure fluctuation in across-wind direction from the flow movement equation.

In this study, we attempt to find an approximate equation for the across-wind fluctuating moment coefficient and spectral density coefficient, which are dependent on gust and wake turbulence, as a function of the aspect ratio H/\sqrt{BD} (where, H is the height of the building) and the side ratio D/B of buildings. In order to estimate the empirical formula, HFFB tests were conducted on fifty-two types of linear-mode rigid models of rectangular prisms with various aspect and side ratios in turbulent boundary-layer flows. Four different aspect ratios and thirteen different side ratios were used.

2. Model and measurement

2.1 Wind model

The wind tunnel tests for the across-wind force were performed in the boundary-layer wind tunnel at the Kumoh National Institute of Technology in Korea. The working section of the tunnel is $1.54 \times 1.3 \times 14$ m size. The tests were carried out under turbulent boundary flows over suburban areas. In order to simulate the boundary-layer flow, spires were set at the entrance to the working section and roughness blocks were placed on the tunnel floor. The characteristics of the 1/400 scale approach-flow boundary-layer wind model are given in Fig. 1. The mean velocity profiles in the turbulent boundary layer flow agree well with the power law (the exponent for this law is 0.22 for suburban areas) categorized in the Korean Building Code 2009.

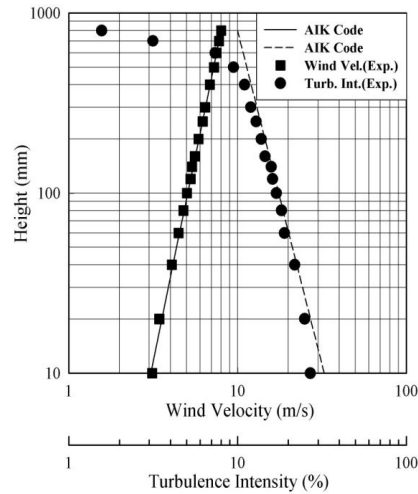


Fig. 1 Profiles of mean velocities and longitudinal turbulence intensities

2.2 Building model

The model scale was 1/400, which was chosen from a comparison of the turbulent scale in the wind tunnel with natural wind. The building models for the tests were constructed from balsa of low weight and strong stiffness, they are therefore considered as linear-mode rigid models. The models had rectangular section, all had the same cross-sectional area of $B \times D = 64 \text{ cm}^2$. Four aspect ratios H / \sqrt{BD} were used $H / \sqrt{BD} = 4, 5, 6$ and 8 . Thirteen side ratios D / B were used $D / B = 1/5, 1/4, 1/3, 1/2, 1/1.5, 1.25/1, 1.5/1, 1/1, 1.25/1, 1.5/1, 2/1, 3/1, 4/1,$ and $5/1$

2.3 Measurement

Fifty-two different building models with rectangular sections were mounted on the HFFB. The model and HFFB were connected together securely at the base. The natural frequency of this system was about 150 Hz, which was high enough for the resonant problem not to occur in this system and for data to be properly measured. The dynamic across-wind forces of the models were measured through HFFB tests.

The conditions for measuring the dynamic wind force were as follows: 1/400 model length scale; 1/4 wind velocity ratio; 1/100 time ratio; 200 Hz sampling frequency; 8th round sampling; and 100 Hz low pass filter cutting frequency.

3. Experimental results and discussion

3.1 Parameters and configurations

The across-wind force data are presented as the mean and standard deviation of the force coefficient, defined along with other parameters as follows

Mean wind force coefficient $C_{FL} = \{ \overline{F_L} / (q_H BH) \}$ (1)

Mean overturning moment coefficient $C_{ML} = \{ \overline{M_L} / (q_H BH^2) \}$ (2)

Fluctuating wind force coefficient $C_{FL}' = \{ \sigma_{FL} / (q_H BH) \}$ (3)

Fluctuating overturning moment coefficient $C_{ML}' = \{ \sigma_{ML} / (q_H BH^2) \}$ (4)

where $\overline{F_L}$ and $\overline{M_L}$ are the mean force and overturning moment, respectively, σ_{FL} and σ_{ML} are the standard deviations of the fluctuating force and overturning moment, respectively, q_H is the dynamic velocity pressure at the top of building H, and ρ is the air density.

3.2 Wind force coefficient

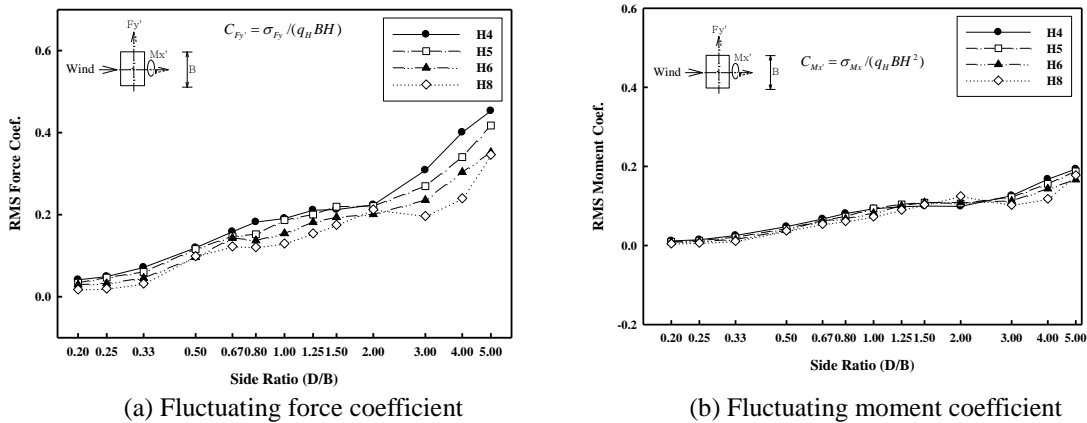


Fig. 2 Across-wind fluctuating force coefficient

Fig. 2 shows the effect of the aspect ratio H/\sqrt{BD} and side ratio D/B on the across-wind fluctuating force coefficient C_{FL}' . With changing aspect ratio H/\sqrt{BD} , the fluctuating force coefficient C_{FL}' has a large value in low-rise buildings but gradually decreases as the building height increases. For different side ratio D/B , the fluctuating force coefficient C_{FL}' tends to increase as D/B increases. In particular, C_{FL}' shows a gradual increase until D/B reaches 2.0, but a rapid increase when D/B exceeds 3.0.

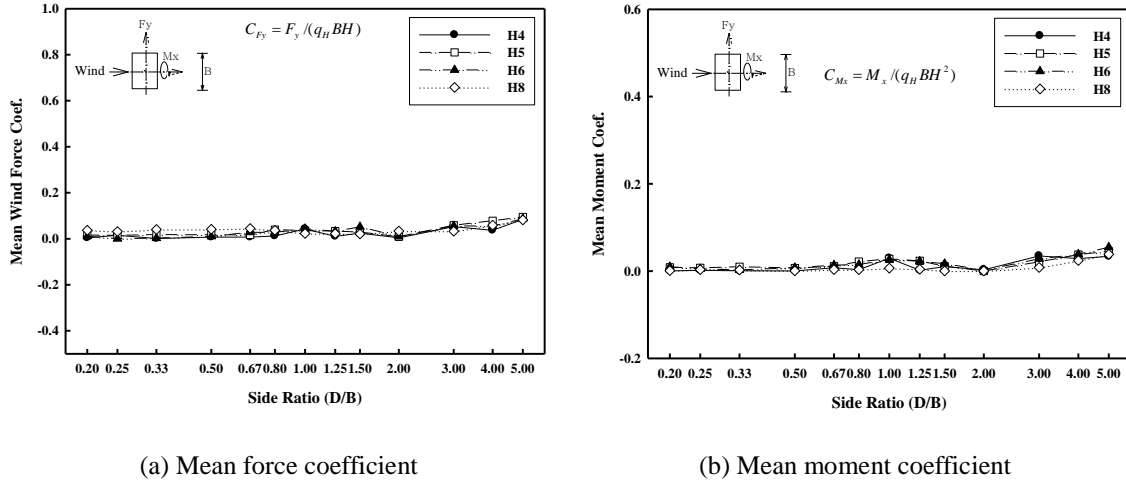


Fig. 3 Across-wind mean force coefficient

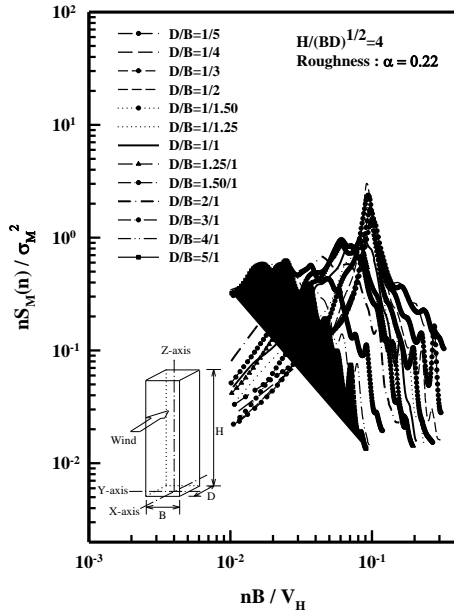
Fig. 3 shows the effect of the aspect ratio H/\sqrt{BD} and side ratio D/B on the across-wind mean force coefficient C_{FL} . The mean wind force coefficients C_{FL} have values of almost zero value regardless of the values of H/\sqrt{BD} and D/B . The reason for this result is that vortex shedding of the same magnitude but opposite direction occurs at the rear of the building.

3.3 Wind force spectral density

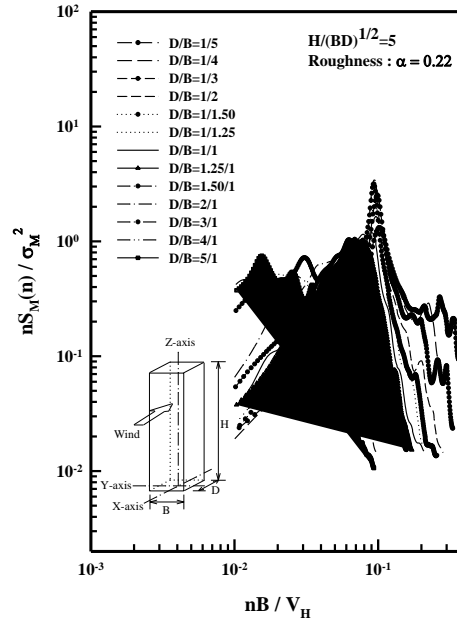
Fig. 4 shows the across-wind fluctuating moment spectral density with respect to the aspect ratio H/\sqrt{BD} as a function of the side ratio D/B and the reduced frequency nB/V_H , where n is the natural frequency of the cylinder and V_H is the wind velocity at the top of building. With changes in the aspect ratio H/\sqrt{BD} , the shapes and band-widths of the spectral density are similar to each other with variation of the side ratios D/B . As the aspect ratio H/\sqrt{BD} increases, the power of the spectral density and the Strouhal number show only small increments.

However, with changes in the side ratio D/B , the spectra present narrow bands. When the side ratio D/B is less than 1.25, there is one significant peak of the resonance by vortex shedding, and the reduced frequency nB/V_H at the spectral peak is about 0.1. This is caused by the vortices from both sides being shed alternately into the wake synchronized with the across wind vibration. The peak heights are comparatively large.

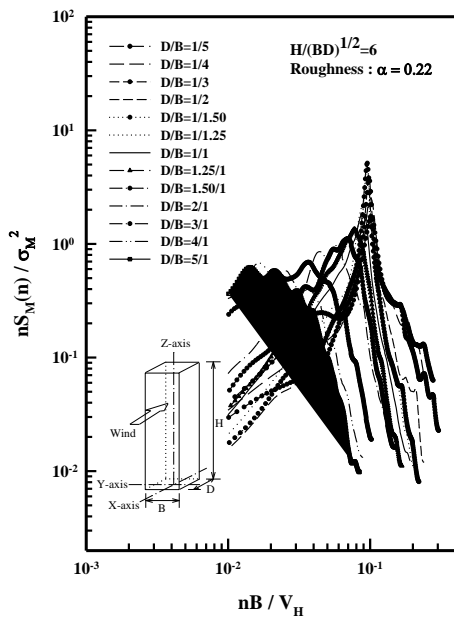
When the side ratio D/B is larger than 1.5, there is a small spectral peak in the region of the reduced frequency nB/V_H between 0.01 and 0.07.



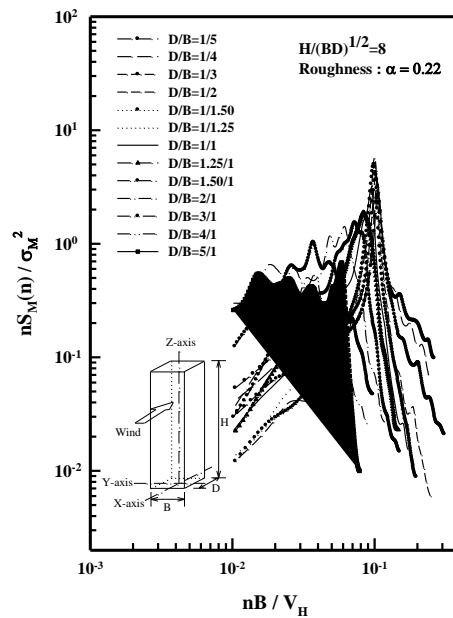
(a) $H / \sqrt{BD} = 4$



(b) $H / \sqrt{BD} = 5$



(c) $H / \sqrt{BD} = 6$



(d) $H / \sqrt{BD} = 8$

Fig. 4 Across-wind fluctuating overturning moment spectral density with various side ratios

Fig. 5 shows the Strouhal Number S_t for the across-wind plotted against the side ratios D/B . In this paper, when the frequency of vortex shedding equals the frequency of the spectral peak n_p , the Strouhal Number S_t , is given by

$$S_t = n_p B / V_H \tag{5}$$

As the aspect ratio H/\sqrt{BD} changes, the Strouhal Number S_t tends to increase gradually in proportion to H/\sqrt{BD} . This means that if the aspect ratio has a large value, resonance may occur in a low wind speed region. However, when the side ratio D/B is larger than 3.0, the tendency of the increments in proportion to H/\sqrt{BD} is not obvious.

As the side ratio D/B changes, S_t is between 0.01 and 0.1 in the low-frequency region and decreases as D/B increases. It is interesting that when D/B is less than 1.0, S_t tends to decrease slowly as D/B increases, but decreases suddenly when D/B exceeds 1.0.

From the tendencies mentioned above, it can be seen that the power spectral density of the fluctuating moment and the Strouhal number are strongly affected by changes in the side ratio D/B , but are only slightly affected by changes in the aspect ratio H/\sqrt{BD} .

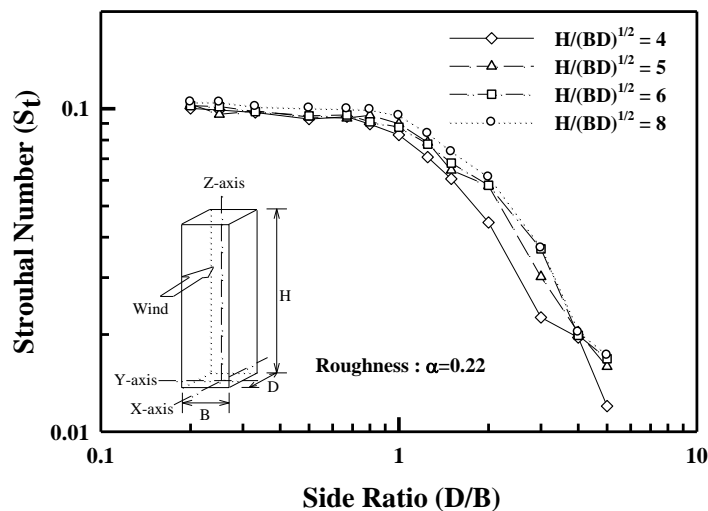


Fig. 5 Strouhal Number S_t for across-wind

4. Empirical formulas

4.1 Fluctuating moment coefficient

Fig. 6 shows the fluctuating overturning moment coefficient C_{ML}' for the across-wind as a function of the aspects ratio H/\sqrt{BD} and the side ratio D/B . The fluctuating overturning

moment coefficient C_{ML}' presents little variation with changes in the aspect ratio H/\sqrt{BD} . However, it shows significant variation with changes in the side ratio D/B . For a side ratio D/B of 2.0, C_{FL}' increases slowly in proportion to D/B , for a side ratio of over 3.0, C_{ML}' increases sharply in proportion to D/B . From these results, it can be seen that the fluctuating overturning moment coefficients C_{ML}' are strongly affected by the side ratio D/B rather than by the aspect ratio H/\sqrt{BD} , so the experimental formula of C_{ML}' can be approximately obtained by dividing the side ratio D/B into two parts as follows

$$C_{ML}' = -0.011(D/B)^3 + 0.0769(D/B)^2 + 0.1795(D/B) - 0.0289$$

(6)

; $[0 < (D/B) < 3.0]$

$$C_{ML}' = 0.0327(D/B) + 0.0164$$

(7)

; $[3.0 \leq (D/B) \leq 5.0]$

Eqs. (6) and (7) have acceptable error ranges of 9.7% and 8.6%, respectively.

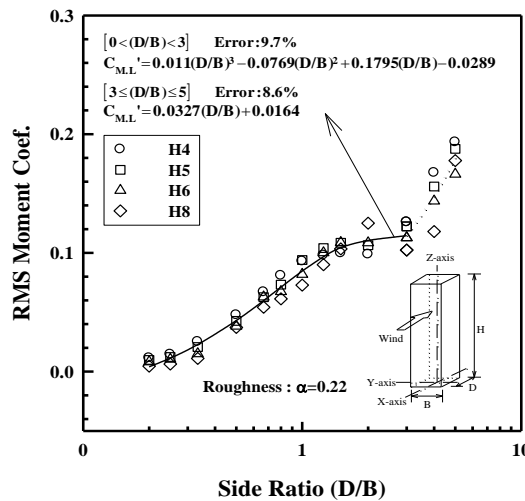


Fig. 6 Generalized across-wind fluctuating overturning moment coefficient

4.2 Fluctuating moment spectral density coefficient

Fig. 7 shows the across-wind fluctuating moment spectral density, for which the reduced frequency takes the form $n\sqrt{BD}/V_H$ instead of nB/V_H . It is, in general, rare to find the natural frequency of a building located in the lower-frequency part of the power spectral peak, so it is important to consider the higher-frequency part of the spectral peak to estimate the dynamic response of a building. Therefore, we mainly consider the higher-frequency part of the spectral

peak to estimate an empirical equation for the power spectra. From the tendency shown in Fig. 7, when side ratio of the model is larger than 3.0, re-attachment occurs, thus the second spectral peak which is smaller than the first one, is appear at the high frequency domain, the experimental formula for the across-wind fluctuating moment spectral density coefficient F can be approximately expressed as follows in according to the value of the side ratio, which was based on the AIJ Recommendations for Loads on Buildings. (AIJ 2004, Marukawa 1992)

$$F = \sum_{j=1}^N \frac{4k_j(1+0.5\beta_j)\beta_j}{\pi} \frac{(n/n_{pj})^2}{\{1-(n/n_{pj})^2\}^2 + 4\beta_j^2(n/n_{pj})^2} \tag{8}$$

$$N = \begin{cases} 1: D/B < 3 \\ 2: D/B \geq 3 \end{cases} \quad \begin{cases} k_1 = 1.00 \\ k_2 = 0.01 \end{cases}$$

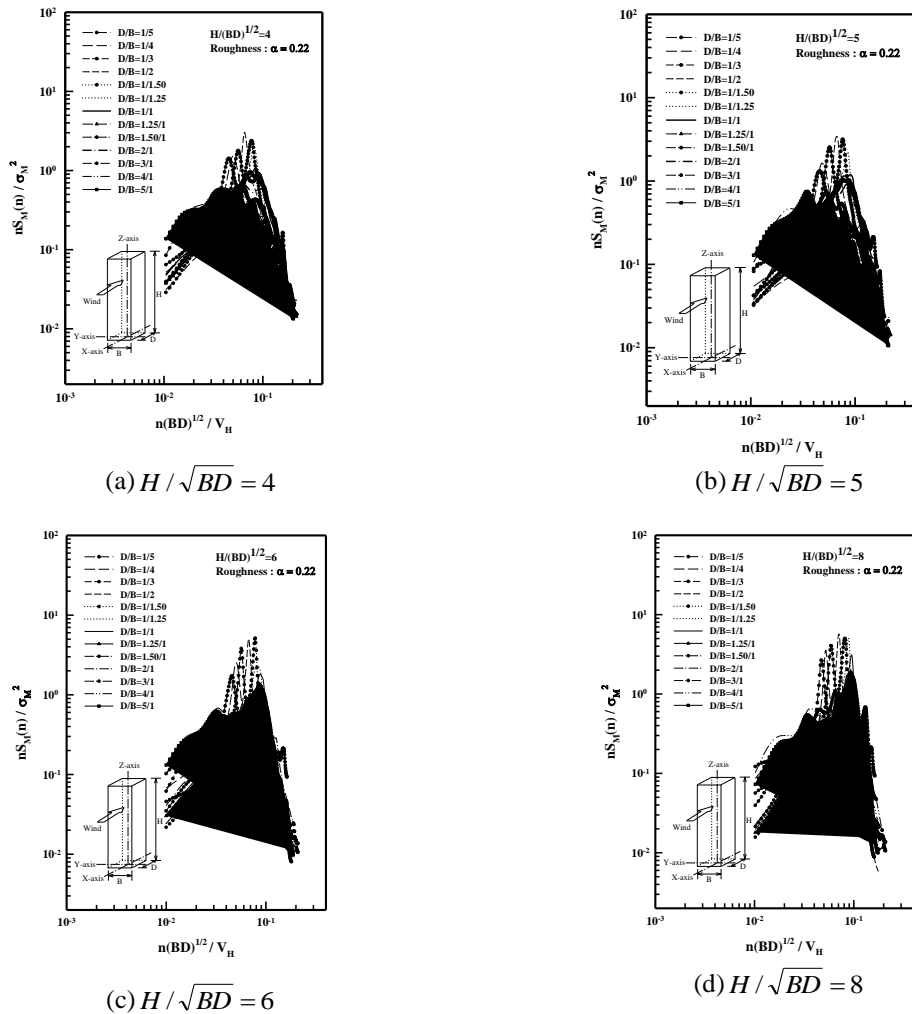


Fig. 7 Across-wind fluctuating overturning moment spectral density for various side ratios

Fig. 8 shows the spectral peak frequency for the aspect ratio H/\sqrt{BD} . In the figure, Exp.(H4) shows the experimental results for the model of aspect ratio 4 acquired from HFFB tests and The.(H4) shows the approximate equation for the model of aspect ratio 4 fitted to the experimental result. The maximum value occurs for a side ratio D/B of about 1.0. On the other hand, the spectral peak frequency has a tendency to become larger with increasing aspect ratio H/\sqrt{BD} . From this figure, approximate equations for the first spectral peak n_{p1} frequency can be obtained according to H/\sqrt{BD} as follows (AIJ 2004)

$$H/\sqrt{BD} = 4 \quad ; \quad n_{p1} = \frac{0.102}{\{1+0.25(D/B)^2\}^{1.1}} \frac{V_H}{B} \tag{9}$$

$$H/\sqrt{BD} = 5 \quad ; \quad n_{p1} = \frac{0.103}{\{1+0.21(D/B)^2\}^{1.1}} \frac{V_H}{B} \tag{10}$$

$$H/\sqrt{BD} = 6 \quad ; \quad n_{p1} = \frac{0.103}{\{1+0.19(D/B)^2\}^{1.1}} \frac{V_H}{B} \tag{11}$$

$$H/\sqrt{BD} = 8 \quad ; \quad n_{p1} = \frac{0.106}{\{1+0.17(D/B)^2\}^{1.1}} \frac{V_H}{B} \tag{12}$$

And as shown in Fig. 9, the second spectral peak frequency n_{p2} can be approximately obtained regardless of the variation of aspect ratio H/\sqrt{BD} as follow (AIJ 2004)

$$n_{p2} = \frac{0.61}{(D/B)^{0.89}} \frac{V_H}{B} \tag{13}$$

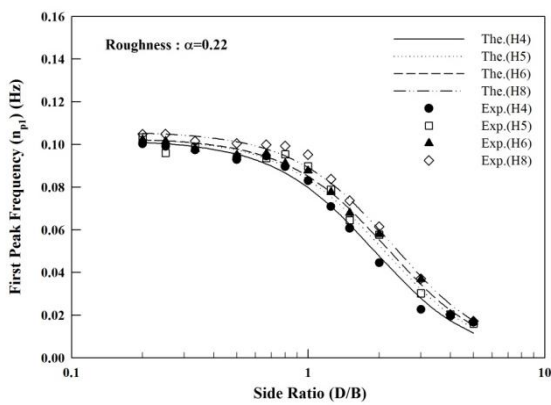


Fig. 8 First spectral peak frequency

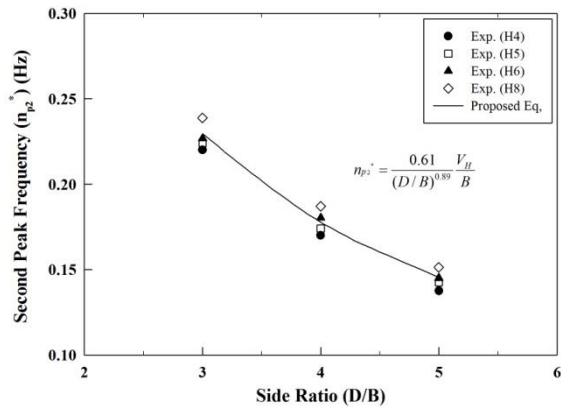


Fig. 9 Second spectral peak frequency

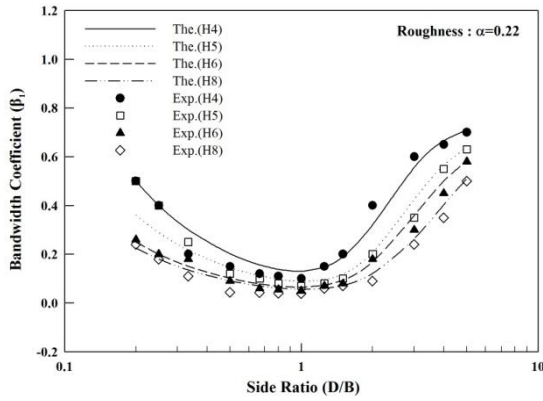


Fig. 10 Coefficient for effective bandwidth of the first spectral peak

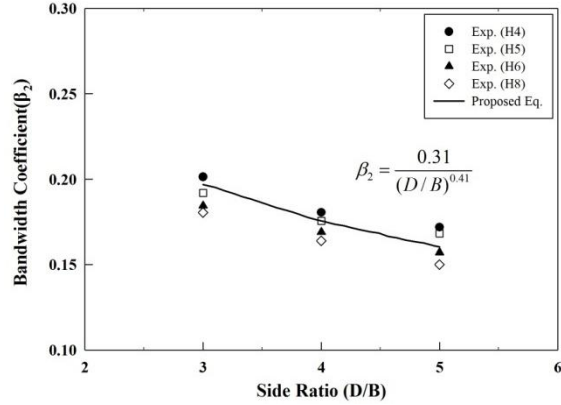


Fig. 11 Coefficient for effective bandwidth of the second spectral peak

Fig. 10 shows the coefficient for the effective bandwidths of the first spectral peak as a function of the side ratios. In this figure, Exp.(H4) shows the experimental results for the model of the aspect ratio 4 and The.(H4) shows an approximate equation for the model of the aspect ratio 4 fitted to the experimental results. The minimum value occurs at a side ratio D/B of about 1.0. On the other hand, the bandwidth has a tendency to become smaller increasing aspect ratio H/\sqrt{BD} . From this figure, an approximate equation for the coefficient of the effective bandwidth of the first spectral peak can be expressed β_1 according to the aspect ratio H/\sqrt{BD} as follows (AIJ 2004)

$$H/\sqrt{BD} = 4 ; \quad \beta_1 = \left\{ \frac{(D/B)^4}{1.32(D/B)^4 + 2(D/B)^2 + 30} \right\} + \frac{0.1}{(D/B)} \quad (14)$$

$$H/\sqrt{BD} = 5 ; \quad \beta_1 = \left\{ \frac{(D/B)^4}{1.32(D/B)^4 + 5(D/B)^2 + 70} \right\} + \frac{0.1}{(D/B)} \quad (15)$$

$$H/\sqrt{BD} = 6 ; \quad \beta_1 = \left\{ \frac{(D/B)^4}{1.35(D/B)^4 + 7.5(D/B)^2 + 60} \right\} + \frac{0.05}{(D/B)} \quad (16)$$

$$H/\sqrt{BD} = 8 ; \quad \beta_1 = \left\{ \frac{(D/B)^4}{1.2(D/B)^4 + 17(D/B)^2 + 75} \right\} + \frac{0.045}{(D/B)} \quad (17)$$

And as shown in Fig. 11, the effective bandwidth of the second spectral peak β_2 can be approximately obtained regardless of the variation of aspect ratio H/\sqrt{BD} as follow (AIJ 2004)

$$\beta_2 = \frac{0.31}{(D/B)^{0.41}} \quad (18)$$

Fig. 12 shows the generalized across-wind fluctuating overturning moment spectral density coefficients F of Eq. (8) for various side ratios D/B . It can be seen that the shape of the spectral density coefficient is slightly affected by the variation of aspect ratio H/\sqrt{BD} , but is strongly affected by the variation of the side ratio D/B . When the side ratio D/B is closer to 1.0, the spectral peak frequency has its maximum value and the spectral bandwidth shows its minimum value (the bandwidth has the narrowest shape).

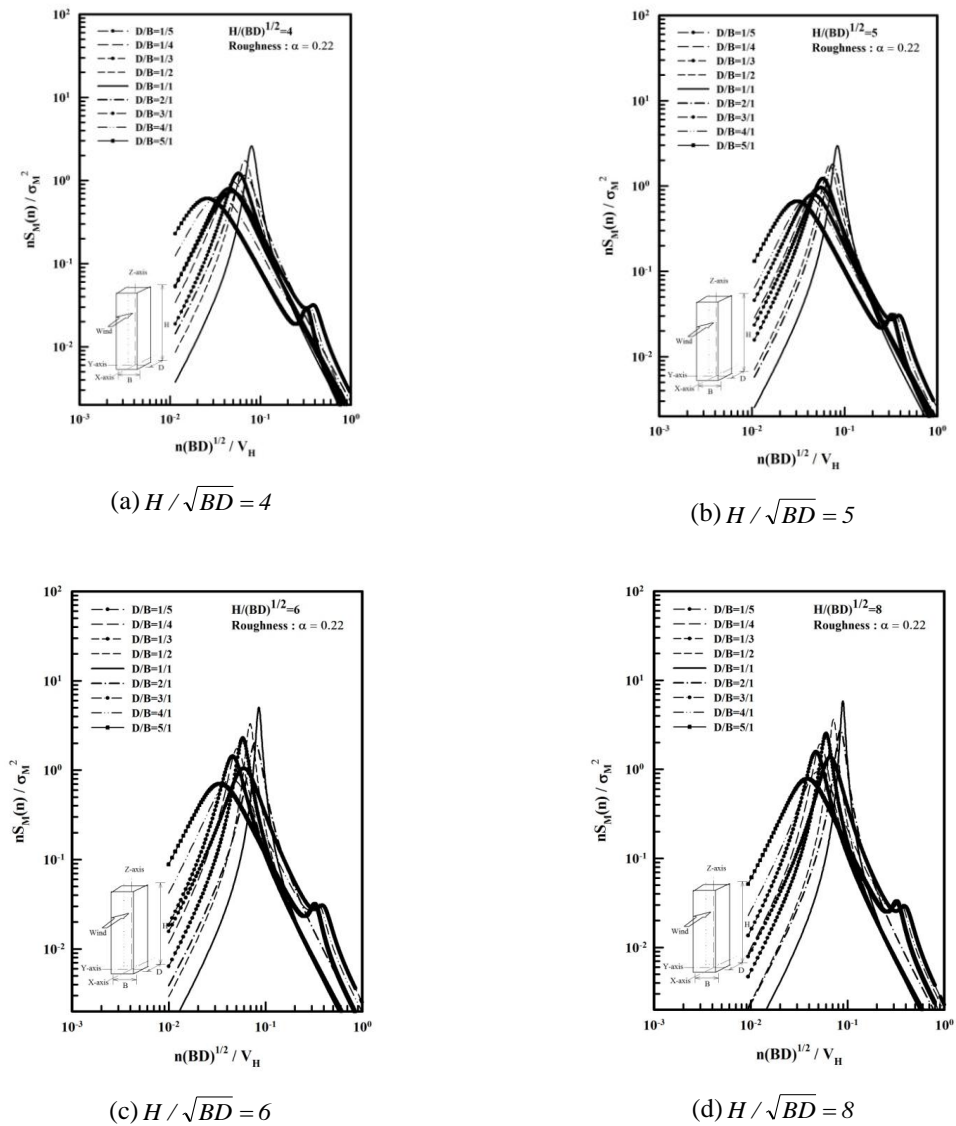


Fig. 12 Generalized across-wind fluctuating overturning moment spectral density coefficient

5. Conclusions

In this investigation, on the basis of the extensive experimental data obtained through wind tunnel tests, an empirical formula for the evaluation of across-wind dynamic loads on rectangular tall buildings has been presented. The formula proposed in this paper is in good agreement with the experimental data. A calculation method based on this empirical formula can be established to estimate the across-wind dynamic responses or dynamic loads of rectangular tall buildings in the frequency domain at the preliminary design stage of the buildings. The main conclusions obtained in this paper are as follows:

(1) The across-wind fluctuating overturning moment coefficients tend to be affected mainly by changes in the side ratio, and only slightly affected by the aspect ratio. Therefore, the empirical equations given by Eqs. (6) and (7) were estimated as a function of the side ratio.

(2) The across-wind fluctuating moment spectral density shows only a small increment as the aspect ratio H/\sqrt{BD} increases. However, it is strongly affected by changes in the side ratio D/B . When the side ratio D/B is under 1.25, there is one significant peak of the resonance by vortex shedding and the reduced frequency nB/V_w at the spectral peak is about 0.1. When the side ratio D/B is over 1.5, there is a smaller spectral peak in the region of the reduced frequency nB/V_H between 0.01 and 0.07. As the side ratio increases, the spectral peak frequency moves into the lower-frequency region.

(3) The Strouhal Number S_f tends to increase gradually in proportion to H/\sqrt{BD} . However, when D/B is larger than 3.0, the tendency of increment in proportion to H/\sqrt{BD} is not obvious. S_f decreases as D/B increases. It is interesting that, when D/B is less than 1.0, S_f tends to decrease slowly as D/B increases, decreases sharply when D/B exceeds 1.0.

(4) The maximum value of the spectral peak occurs for a side ratio D/B of about 1.0. On the other hand, the spectral peak frequency has a tendency to increase with the increasing aspect ratio H/\sqrt{BD} .

(5) The minimum value of the effective bandwidth of the spectra occurs for a side ratio D/B of about 1.0. On the other hand, the bandwidth has a tendency to decrease with increasing of aspect ratio H/\sqrt{BD} .

(6) It can be seen that the shape of the spectral density coefficient is slightly affected by the variation of aspect ratio H/\sqrt{BD} , but is strongly affected by the variation of the side ratio D/B . When the side ratio D/B is closer to 1.0, the spectral peak frequency has its maximum value and the spectral bandwidth shows its minimum value.

(7) For the wind induced response of buildings, it is in general rare for the natural frequency of a building to be located in the lower-frequency part of the power spectral peak, so we mainly consider the higher-frequency part of the spectral peak to estimate empirical equations for the spectral density. Empirical equations for the across-wind fluctuating moment spectral density coefficient are given by Eqs. (8) to (18).

Acknowledgments

This research (03R&D C04-01) was supported financially by the Ministry of Construction & Transportation of South Korea and the Korea Institute of Construction and Transportation

Technology Evaluation and Planning, and the authors are grateful to the authorities for their support.

References

- Architectural Institute of Japan (2004), *AIJ Recommendations for Loads on Buildings*.
- Architectural Institute of Korea (2009), *Korean Building Code and Commentary*.
- Davenport, A.G. (1962), "The response of slender line-like structures to a gusty wind", *Proc. I.C.E.*, **23**(3), 449-472.
- Nan, G.E., Abio, H. and Xiyuan, Z. (2007), "Evaluation of across-wind dynamic response for rectangular high rise buildings", *Eng. Mech.*, **24**(10), 80-86.
- Nan, G.E., Abio, H. and Xiyuan, Z. (2008), "Evaluation of dynamic response induced by turbulence in across-wind direction on high rise buildings", *Chinese J. Appl. Mech.*, **25**(2), 218-223.
- Ha, Y.C. and Kim, D.W. (2002), "Wind tunnel test study on the effective elevation and plan shapes of super high-rise buildings for resisting wind-induced responses", *J. Arch. Inst. Korea*, **18**(9), 93-100 (in Korean).
- Ha, Y.C. (2004), "Estimation of the across-wind fluctuating moment and spectral density coefficient of rectangular tall buildings with various side ratios", *Proceedings of the 11th Australian Wind engineering Society Workshop*, Darwin.
- Ha, Y.C. and Kim, D.W. (2004), "Characteristics of the across-wind fluctuating force and spectral density of rectangular high-rise buildings with various side ratios", *Proceedings of the CTBUH 2004 Seoul Conference*, Seoul, Korea.
- Ha, Y.C., Kim, D.W., Choi, S.G and Kil, Y.S. (2005), "Characteristics of the across-wind force of rectangular tall buildings with various roughness", *J. Wind Eng. Inst. Korea*, **9**(1), 79-85 (in Korean)
- Kareem, A. (1989), "Fluctuating wind loads on buildings", *J. Eng. Mech. - ASCE*, **108**(6), 1086-1102.
- Kawai, H. (1992), "Vortex induced vibration of tall buildings", *J. Wind Eng. Ind. Aerod.*, **41**(1-3), 117-128.
- Kim, Y.M, You, K.P. and Ko, N.H (2008), "Across-wind responses of an aeroelastic tapered tall building", *J. Wind Eng. Ind. Aerod.*, **96**(8-9), 1307-1319.
- Marukawa, H., Ohkuma, T. and Momomura, Y. (1992), "Across-wind and torsional acceleration of prismatic high rise buildings", *J. Wind Eng. Ind. Aerod.*, **41-44**, 1139-1150.
- Melbourne, W.H. (1975), "Tall rectangular building response to cross-wind excitation", *Proceedings of the 4th International Conference on Wind Effects on Buildings & Structures*, London, UK.
- National Building Code of Canada (2005), *Part 4 Structural Design*.
- Liang, S, Liu, S, Li, Q.S, Zhang, L and Gu, M. (2002), "Mathematical model of acrosswind dynamic loads on rectangular tall buildings", *J. Wind Eng. Ind. Aerod.*, **90**(12-15), 1757-1770.
- Liang, S, Liu, S, Li, Q.S, Zou, L.H. and Wu, J.R. (2005), "Simplified formulas for evaluation of across-wind dynamic responses of rectangular tall buildings", *Wind Struct.*, **8**(3), 197-212.
- Lin, N, Letchford, C, Tamura, Y, Liang, B. and Nakamura, O. (2005), "Characteristics of wind forces acting on tall buildings", *J. Wind Eng. Ind. Aerod.*, **93**(3), 217-242.
- Quan, Y. and Gu, M. (2006) "Analytical method of across-wind response and equivalent static wind loads of high-rise buildings", *Eng. Mech.*, **23**(9), 84-88.
- Vickery, B.J. (1966), "On the assessment of wind effects on elastic structures", *C. E. Trans., Inst. Aust.*, 183-192.
- Vickery, B.J. (1972), "Lift or across-wind response of tapered stacks", *Proceedings of the ASCE*, **98**(1), 1-20.